Environmental Science & Technology

Article

pubs.acs.org/est

Reactive Uptake of an Isoprene-Derived Epoxydiol to Submicron Aerosol Particles

Cassandra J. Gaston,[†] Theran P. Riedel,[‡] Zhenfa Zhang,[‡] Avram Gold,[‡] Jason D. Surratt,[‡] and Joel A. Thornton*,[†]

[†]Department of Atmospheric Sciences, University of Washington, Seattle, Washington 98195 United States

[‡]Department of Environmental Sciences and Engineering, Gillings School of Global Public Health, University of North Carolina, Chapel Hill, North Carolina 27599 United States

Supporting Information

ABSTRACT: The reactive uptake of isoprene-derived epoxydiols (IEPOX) is thought to be a significant source of atmospheric secondary organic aerosol (SOA). However, the IEPOX reaction probability (γ_{IEPOX}) and its dependence upon particle composition remain poorly constrained. We report measurements of γ_{IEPOX} for *trans*-β-IEPOX, the predominant IEPOX isomer, on submicron particles as a function of composition, acidity, and relative humidity (RH). Particle acidity had the strongest effect. γ_{IEPOX} is more than 500 times greater on ammonium bisulfate ($\gamma \sim 0.05$) than on ammonium sulfate ($\gamma \leq 1 \times 10^{-4}$). We could accurately predict γ_{IEPOX} using an acid-catalyzed, epoxide ring-opening mechanism and a high Henry's law coefficient (1.7×10^8 M/atm). Suppression of γ_{IEPOX} was observed on particles containing both ammonium bisulfate and poly(ethylene glycol) (PEG-300), likely due to diffusion and solubility limitations within a PEG-300 coating, suggesting that IEPOX uptake could be self-limiting. Using the measured uptake kinetics, the predicted atmospheric lifetime of IEPOX is a few hours in the presence of highly acidic particles (pH < 0) but is greater than 25 h on less acidic particles (pH > 3). This work highlights the importance of aerosol acidity for accurately predicting the fate of IEPOX and anthropogenically influenced biogenic SOA formation.

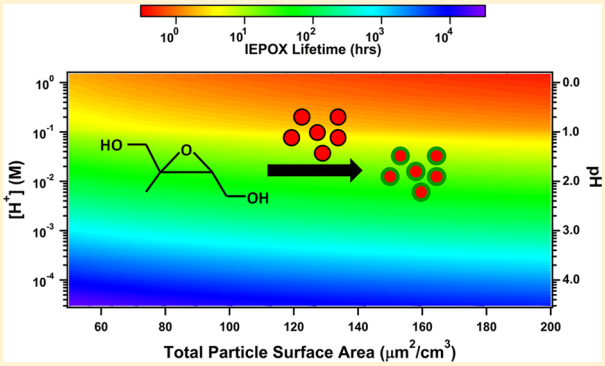

1. INTRODUCTION

Atmospheric fine particulate matter influences the global climate directly by scattering and absorbing incoming solar radiation and indirectly by affecting cloud properties. Both the size and chemical composition of particles influence their interaction with radiation and cloud-forming abilities.[1−4] Therefore, accurate representation of these two parameters in global climate models is needed to quantify the effects of aerosol particles in both space and time. Carbonaceous material is a major component of atmospheric aerosol in the submicron size range.[5−13] Recent work has shown that much of this organic aerosol (OA) arises from secondary processes involving the conversion of volatile organic compounds (VOC) into secondary organic aerosol (SOA), and that models often under-predict observed OA mass concentrations.[12,14−16] Moreover, some models better predict observed OA when SOA is assumed to form kinetically via reactive uptake or from the irreversible condensation of low-volatility organic compounds, with a significant enhancement due to anthropogenic activities.[17−20]

A significant fraction of SOA arises from biogenic as opposed to anthropogenic VOC precursors.[9,21] Even a relatively low yield of SOA from the oxidation of isoprene, the most ubiquitous nonmethane VOC emitted to the atmosphere,[22] has the potential to contribute a major fraction of SOA.[7,9,23−25] Under low nitric oxide (NO) conditions, isoprene reacts with hydroxyl radicals (OH) to produce organic peroxy radicals that react with hydroperoxyl radicals (HO_2) to form isomeric hydroxy hydroperoxides (ISOPOOH). As first shown by Paulot et al.,[26] reaction of ISOPOOH with OH produces isomeric epoxydiols (IEPOX) in high yields.[26] Evidence from chamber studies and field measurements suggest that IEPOX is a key gas-phase intermediate leading to the formation of compounds that contribute to the biogenic SOA burden including 2-methyltetrols, organosulfates, C_5-alkene triols, and 3-methyltetrahydrofuran-3,4-diols.[7,9,23−35]

Using surrogate compounds, numerous studies have shown that epoxides are efficiently taken up by acidic aerosol leading to the formation of organosulfates and polyols via a ring-opening reaction mechanism.[25,32,36,37] Recent measurements of SOA production from authentic *cis*-β-IEPOX and a racemic mixture of diastereomeric δ-IEPOX standards on chamber-derived aerosol confirm that higher SOA yields are observed on

Received: July 15, 2014
Revised: September 5, 2014
Accepted: September 10, 2014
Published: September 10, 2014

 © 2014 American Chemical Society

acidic aerosol.[30] In contrast, ambient measurements have shown weak or nonexistent correlations between IEPOX-derived SOA and metrics of particle acidity.[27,38,39] Causes of this discrepancy include artificially high acidities used in chamber studies and poor estimation of atmospheric aerosol acidity, for example, by titration of ambient aerosol acidity during sampling.[38,40] In addition, other catalysts could be important factors for the reactive uptake of IEPOX on less acidic particles.[41−44] Understanding the factors affecting IEPOX reactive uptake to atmospheric particles is necessary for determining the mechanism and quantity of isoprene-derived SOA.

We present laboratory measurements of the reactive uptake of *trans*-β-IEPOX, the predominant IEPOX isomer from the OH-initiated oxidation under low-NO conditions,[45] onto submicron aerosol particles using an entrained aerosol flow reactor combined with chemical ionization mass spectrometry (CIMS). Because previous studies have shown that the presence and position of certain substituents, such as hydroxyl groups, can significantly impact epoxide ring-opening kinetics, the use of an authentic IEPOX standard allows for accurate quantification of the reaction kinetics of IEPOX in aerosol particles.[36,46] Further, such experiments can probe a range of atmospherically relevant RH and particle compositions, including the highly ionic solutions accessible only with metastable particles at RH <∼80%. This study aims to (i) quantify the net reactive uptake kinetics of *trans*-β-IEPOX on particles with different chemical compositions, (ii) determine the importance of liquid water content and particle acidity on IEPOX reactive uptake, and (iii) use the observations to constrain key variables, such as the Henry's law coefficient and aqueous phase reaction rate constants, needed to parametrize IEPOX reactive uptake in models. The implications of our findings for the formation of SOA from IEPOX are also briefly discussed.

2. METHODS

Measurements of the reactive uptake of *trans*-β-IEPOX were made using an entrained aerosol flow tube coupled to an iodide adduct chemical ionization mass spectrometer (CIMS). The flow tube, aerosol generation, and CIMS have been described in detail previously.[47−51] We provide summaries here relevant to the IEPOX system.

Aerosol Generation and Characterization. Similar to previous studies, aerosols were generated with a constant output atomizer (TSI Inc., Model 3076) from dilute solutions (0.085 wt %) that are atomized and conditioned to a specific RH before entering the flow tube.[47−51] Ammonium bisulfate (Sigma-Aldrich, 99.99% purity), ammonium sulfate (Sigma-Aldrich, ≥99% purity), sulfuric acid (ACROS, 95% purity), and poly(ethylene glycol) with an average molecular weight of 300 g/mol (chemical formula $H(OCH_2CH_2)_nOH$) (Sigma-Aldrich) were used as the aerosol components. The atomizer output was diluted and conditioned by mixing 5 standard liters per minute (slpm) of humidified ultrahigh purity (UHP) N_2 with the atomizer output. The humidity of the aerosol flow was adjusted to the desired RH in a conditioning region, and RH was measured with a Vaisala humidity probe (accuracy ±2%) just upstream of the flow reactor. A schematic of the experimental setup can be found in the Supporting Information(Figure S1). The resulting particle pH was calculated using the aerosol inorganic model (AIM II)[52] and ranged from −0.3 to +4.6. We assume all particles remain deliquesced, supersaturated solutions in the flow reactor.

Particle size distributions and total surface area concentrations (S_a) at the flow tube exit were measured using a scanning mobility particle sizer (SMPS) consisting of a differential mobility analyzer (DMA) and condensation particle counter (TSI Inc.). S_a typically ranged from 0.4×10^{-4} to 8.6×10^{-4} cm^2/cm^3. Particles were conditioned to approximately 30%, 50%, or 70% RH prior to entering the flow tube. To ensure that the measured S_a was representative of the S_a in the flow tube, the DMA sheath flow was conditioned to the appropriate RH by sampling from the flow reactor for ∼1 h prior to the start of the experiment. The S_a at the flow tube entrance was typically within 10% of that measured at the flow tube exit.

IEPOX Synthesis, Delivery, and Detection. Authentic *trans*-β-IEPOX standards were synthesized using the method of Zhang et al.,[53] and 20 mg aliquots dissolved in 4 mL of ethyl acetate (Macron Fine Chemicals, 99.5% purity) were stored at −30 °C until use. Aliquots of ∼0.25 mL of the dissolved *trans*-β-IEPOX were placed in a glass bulb kept at room temperature (22−25 °C). *trans*-β-IEPOX vapor was entrained into 5−50 sccm of UHP N_2 that passed over the headspace and into a 1/8 in. OD Teflon tube inserted through a stainless steel movable injector in the flow reactor. *trans*-β-IEPOX was detected using iodide adduct CIMS[54] as a cluster with iodide, $I\cdot(IEPOX)^-$ at m/z 244.9, with the same instrument described in Lopez-Hilfiker et al.[49] Ethyl acetate was chosen as the solvent for IEPOX because it is aprotic, unlikely to promote the hydrolysis of IEPOX prior to reaction in the flow tube, has a low Henry's law constant and, therefore, is unlikely to partition into the aerosol and affect particle composition, and is not detected by the CIMS. Thus, the use of ethyl acetate as solvent is unlikely to affect our results. The composition of $I\cdot(IEPOX)^-$ was confirmed to be $I\cdot C_5H_{10}O_3^-$ by sampling the headspace with an iodide adduct high-resolution time-of-flight chemical ionization mass spectrometer (HR-ToF-CIMS),[55] see Figure S2 (Supporting Information).

Determination of γ_{IEPOX}. Measurements of the particle-phase loss rate of *trans*-β-IEPOX relative to its gas-phase collision rate with particles, that is, the IEPOX reaction probability (γ_{IEPOX}), were conducted in either a 3 or 6 cm inner diameter (ID) Pyrex tube, both having a length of 90 cm and inner walls coated with halocarbon wax. A constant 3 slpm of the conditioned particle flow was continuously drawn through the flow reactor using a critical orifice located at the flow tube exit that also served as the sample entrance to the low pressure ionization region of the CIMS and the sample flow drawn by the SMPS. The interaction time between *trans*-β-IEPOX and particles was set by the movable injector position in the flow reactor and the bulk flow velocity. Measurements were limited to the central 50 cm of the flow reactor to remain within well-mixed, laminar flow conditions (Reynold's number ∼69−138).

Different methods were used to determine γ_{IEPOX}: (i) decay of *trans*-β-IEPOX versus interaction time with particles, and (ii) pseudo-particle modulation. Representative measurements using these techniques are shown in Figure S3 of the Supporting Information, and detailed descriptions of these approaches have been published previously.[47−50] We also used the particle modulation method; however, particle modulation involves a fixed injector position in the flow tube while modulating the particle source on and off[56] and may reflect both nonreactive partitioning and heterogeneous chemical loss,

while observation of a time-dependent uptake via the pseudo-particle modulation and/or decay methods indicates that a chemical reaction is actually occurring between the gas and particles driving a net continuous flux to the particle phase. Thus, the results presented in this study focus on the decay and pseudo-particle modulation techniques. Results from the particle modulation technique are included in Table S1 of the Supporting Information to gain insight into cases where partitioning, but no reactive uptake, is observed. In the decay method, the injector is moved in 10 cm increments from the bottom 20 cm to the top 70 cm of the flow tube while maintaining constant S_a and RH to vary the reaction time between *trans*-β-IEPOX and the generated aerosols. Sequential control runs are performed with and without particles to separate the effects of reactor walls. The slope of the natural log of *trans*-β-IEPOX signal versus interaction time yields a pseudo-first order rate coefficient, k_{obs} or k_{wall}, in the presence or absence of particles, respectively (Figure S3a, Supporting Information). The pseudo-first-order reaction rate coefficient for *trans*-β-IEPOX uptake to particles, k_{het}, is then the difference between k_{obs} and k_{wall}.

In the pseudo-particle modulation technique, the injector is repeatedly moved directly between the top and bottom of the flow reactor (Figure S3b, Supporting Information), without additional increments in order to measure multiple values of k_{het} within one sampling period. We used this approach for systems where first-order kinetics were confirmed. The pseudo-first-order reaction rate coefficient for *trans*-β-IEPOX uptake to particles, k_{het}, is then determined from

$$k_{\mathrm{het}} = -\left(\frac{1}{t_{\mathrm{res}}}\right)\ln\left(\frac{[\mathrm{IEPOX}]_{\mathrm{injector\ top}}}{[\mathrm{IEPOX}]_{\mathrm{injector\ bottom}}}\right) \quad (1)$$

where t_{res} is the interaction time between *trans*-β-IEPOX and particles, which ranged between 7 and 28 s.

In all cases, γ_{IEPOX} is calculated using eq 2

$$\gamma_{\mathrm{IEPOX}} \approx \frac{4k_{\mathrm{het}}}{\omega S_{\mathrm{a}}} \quad (2)$$

where ω represents the mean molecular speed of *trans*-β-IEPOX. Equation 2 neglects gas-phase diffusion limitations to reactive uptake, which are typically small (<10%) for the γ_{IEPOX} and particle sizes reported here.[57] The k_{het} were corrected for nonplug flow conditions ("Brown" correction).[58]

The values of γ_{IEPOX} reported here are the means of five independent determinations, and the quoted uncertainties are 95% confidence intervals associated with the measured variation in the determinations. However, we also expect the possibility of undetected systematic errors in the measurements which could bias the results, possibly as much as a factor of 2. For example, a small quantity of residual *trans*-β-IEPOX signal remained in the instrument well after the uptake experiments. This "background" level of *trans*-β-IEPOX (typically ~18%) was measured after each uptake experiment and subtracted from the total signal measured during the γ_{IEPOX} determinations. In addition, for each new interaction time probed, the IEPOX signal evolved slowly over the course of minutes before achieving steady state, likely due to equilibration with the walls of the flow tube and sampling apparatus (see, for example, Figure S3, Supporting Information). We assume the steady-state value is the most appropriate measure to use in the analysis.

3. RESULTS AND DISCUSSION

γ_{IEPOX} Uptake Kinetics and the Role of Particle Acidity. The effect of aerosol acidity was a dominant factor in the reactive uptake of *trans*-β-IEPOX. Measurements of the decay of *trans*-β-IEPOX signal plotted on a log-scale versus injector position (proportional to reaction time) are shown in Figure 1

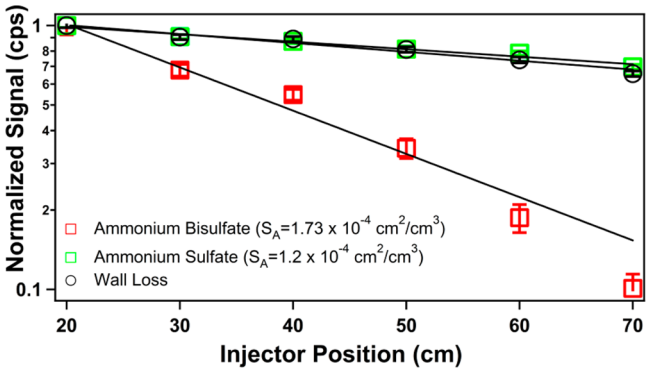

Figure 1. *trans*-β-IEPOX signal vs injector position for ammonium bisulfate (red squares), ammonium sulfate (green squares), and a particle-free, wall loss measurement (black circles) at 50% RH using the full-decay method.

for experiments with and without ammonium bisulfate or ammonium sulfate particles present at 50% RH. The linearity implies pseudo-first-order kinetics. The resulting values of k_{het} after removing loss to the reactor walls are 0.09 ± 0.03 and $1 \times 10^{-3} \pm 0.004\ s^{-1}$ for ammonium bisulfate and ammonium sulfate, respectively (k_{wall} = 0.014 ± 0.006 and 0.013 ± 0.005 s^{-1}, respectively). Equation 2 then gives γ_{IEPOX} values of 0.09 ± 0.03 and $2 \times 10^{-4} \pm 9 \times 10^{-4}$ (Table 1, Figure 1). Averaging the results of the decay and pseudo-particle modulation techniques (see the Supporting Information, Table S1), γ_{IEPOX} is 0.07 ± 0.03 on ammonium bisulfate (Table 1).

We were unable to reliably detect reactive loss of IEPOX on ammonium sulfate. The particle modulation method clearly indicated IEPOX partitioning to ammonium sulfate, but the decay method demonstrated this partitioning was not reactive on the flow reactor time scales. Our best estimate of γ_{IEPOX} on ammonium sulfate is $2 \times 10^{-4} \pm 9 \times 10^{-4}$, which is at least 1 order of magnitude smaller than on ammonium bisulfate and likely below our detection limit, estimated to be $\sim 4 \times 10^{-4}$ from the variation in measured wall loss rates.

Ammonium bisulfate particles have only slightly higher estimated liquid water content than ammonium sulfate particles at 50% RH, (25.7 M vs 24.1 M H_2O based on AIM II), while ammonium bisulfate particles are estimated to be much more acidic than ammonium sulfate particles (pH −0.26 vs 4.63, respectively) implying that differences in particle acidity probably account for the higher γ_{IEPOX} uptake observed for ammonium bisulfate. Consistent with this explanation, acidifying ammonium sulfate particles to pH 1 and pH 0.5 by adding additional H_2SO_4 to the atomizer solution resulted in γ_{IEPOX} of 0.010 ± 0.005 and 0.030 ± 0.008, respectively (Figure 2 and Table 1). These results show a sharp decrease in γ_{IEPOX} for pH > 3.

Role of Liquid Water Content. As noted above, aerosol liquid water played a minor role for γ_{IEPOX} compared to particle acidity in this work. This conclusion is supported by measurements using ammonium bisulfate particles at 30%, 50% and 70% RH, which show that γ_{IEPOX} decreases with RH

Table 1. Relative Humidity (RH), Total Particle Volume/Surface Area Ratios (V/S_a), Technique Used To Determine γ_{IEPOX} and γ_{IEPOX} for Ammonium Bisulfate, Ammonium Sulfate, Acidified Ammonium Sulfate, and Mixtures of Ammonium Bisulfate and PEG[a]

compd	RH (%)	V/S_a (cm)	technique	γ_{IEPOX}
ammonium bisulfate (ABS)	30	4.58e−6	pseudo-particle modulation	0.10 ± 0.01
	50	4.74e−6	pseudo-particle modulation and full decay	0.07 ± 0.03
	70	5.51e−6	pseudo-particle modulation	0.06 ± 0.01
ammonium sulfate	50	3.70e−6	full decay	2e-4 ± 9e-4
ammonium sulfate/H_2SO_4, estimated pH 0.5	50	5.09e−6	pseudo-particle modulation	0.030 ± 0.008
ammonium sulfate/H_2SO_4, estimated pH 1	50	4.11e−6	pseudo-particle modulation	0.010 ± 0.005
ABS/PEG (χ_{PEG} = 0.21)	30	4.40e−6	pseudo-particle modulation	0.080 ± 0.002
ABS/PEG (χ_{PEG} = 0.34)	30	4.75e−6	pseudo-particle modulation	0.080 ± 0.004
ABS/PEG (χ_{PEG} = 0.21)	50	5.90e−6	pseudo-particle modulation	0.050 ± 0.002
ABS/PEG (χ_{PEG} = 0.34)	50	6.95e−6	pseudo-particle modulation	0.040 ± 0.005
ABS/PEG (χ_{PEG} = 0.46)	50	6.08e−6	pseudo-particle modulation	0.020 ± 0.001
ABS/PEG (χ_{PEG} = 0.56)	50	6.68e−6	pseudo-particle modulation	0.020 ± 0.003
ABS/PEG (χ_{PEG} = 0.72)	50	7.40e−6	pseudo-particle modulation	0.010 ± 0.003
ABS/PEG (χ_{PEG} = 0.56)	70	5.61e−6	pseudo-particle modulation	0.002 ± 0.001

[a]The stated uncertainties for γ_{IEPOX} are 95% confidence intervals.

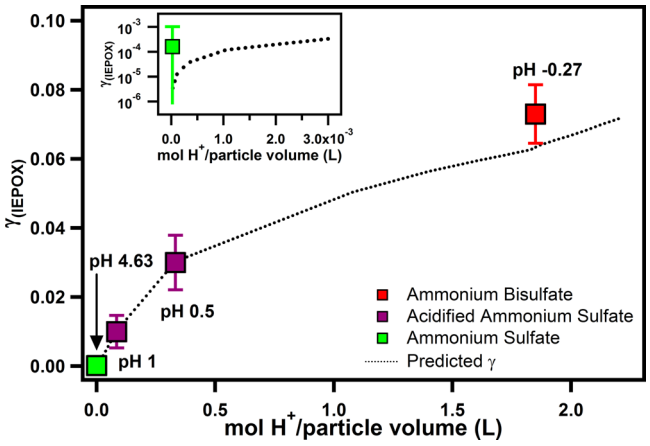

Figure 2. Reactive uptake of *trans*-β-IEPOX as a function of aerosol proton concentration predicted from the AIM II model for ammonium bisulfate (red squares), pure ammonium sulfate (green squares), and ammonium sulfate acidified to pH 0.5 and 1 (purple squares). Inset is a closer view of the uptake on pure ammonium sulfate. Also shown is the predicted reactive uptake assuming the parameters presented in Eddingsaas et al.[36] and using a modified version of the parametrizations presented in Anttila et al.,[62] Bertram and Thornton,[47] and Gaston et al.[48] (black dotted line).

from 0.10 ± 0.01 at 30% RH to 0.06 ± 0.01 at 70% RH (Table 1, Figure 3). Our finding that uptake decreases with increased liquid water content is consistent with that of Nguyen et al.[44]

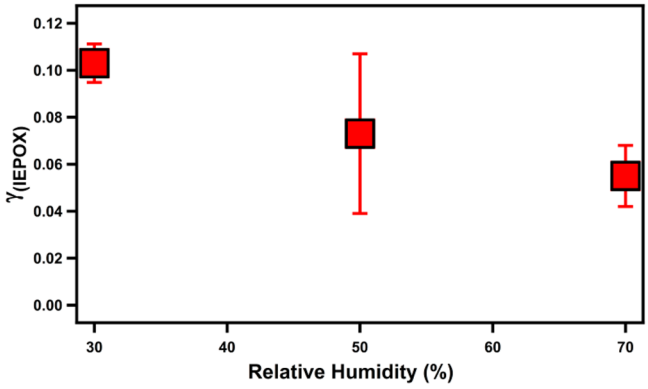

Figure 3. Reaction probability of *trans*-β-IEPOX on ammonium bisulfate particles vs RH.

Modeled particle liquid water contents differed by a factor of 3 across this RH range: 13.6, 25.7, and 36.5 M, respectively. The decrease in γ_{IEPOX} can be explained primarily by the corresponding decrease in proton donor activity and a decrease in the Henry's law constant of IEPOX associated with dilution, an observation that is consistent with previous work where the partitioning of glyoxal was found to decrease as the ionic strength of bulk solutions decreased.[59] A decrease in nucleophilic activity associated with dilution due to increased liquid water content could also be playing a minor role.

Further insight into the role of composition was obtained from the use of the different techniques for determining the uptake on different particle types (NaCl and $MgCl_2$). γ_{IEPOX} for ammonium bisulfate was similar for the three different approaches. However, for nonacidified compositions, uptake of *trans*-β-IEPOX measured by full decay or pseudo-particle modulation yielded much smaller values of γ_{IEPOX} relative to particle modulation (Table S1, Supporting Information). For example, measurement of IEPOX uptake onto $MgCl_2$ particles with the full decay and pseudo-particle modulation techniques was indistinguishable from loss to the reactor walls, similar to our observation for ammonium sulfate; however, γ_{IEPOX} for $MgCl_2$ particles was large for experiments using particle modulation (Table S1, Figure S4, Supporting Information), indicating that *trans*-β-IEPOX largely partitions to ammonium sulfate and $MgCl_2$ particles without undergoing a chemical loss on the time scale of the flow reactor residence time. The time scale to achieve equilibrium partitioning for ∼100 nm size particles should be milliseconds, essentially instantaneous for our experiments.

These results highlight several points. First, particle modulation at constant interaction time produces artificially high values of γ for gases that are less chemically reactive than they are water-soluble, such as *trans*-β-IEPOX. Second, our results for $MgCl_2$ particles show enhanced partitioning of *trans*-β-IEPOX relative to ammonium sulfate and NaCl, the reasons for which remain unclear. Possible explanations include the higher ionic strength and/or nucleophilic activity of $MgCl_2$ aerosols compared to NaCl aerosols, which can increase the Henry's law coefficient (H_{aq}) of water-soluble gases[59,60] and/or strong interactions between Mg^{2+} and organic compounds, in particular, oxygen-containing moieties such as diols.[44,61] Further investigation into this issue is warranted. Third, the substantial change in IEPOX steady-state signal in the presence of these nonacidic particles suggests a large Henry's law

constant and a potential role for solubility-driven partitioning of IEPOX as a non-negligible SOA source.

Predictions of γ_{IEPOX} Using an Acid-Catalyzed Mechanism. The dependence of γ_{IEPOX} on particle acidity supports the use of a parametrization based on an acid-catalyzed, epoxide ring-opening mechanism. Therefore, we used a modified resistor model[47,48,62] with constraints on epoxydiol solubility and reactivity from Eddingsaas et al.[36] to model our results. γ_{IEPOX} was calculated using eqs 3 and 4

$$\frac{1}{\gamma} = \frac{R_p\omega}{4D_g} + \frac{1}{\alpha} + \frac{1}{\Gamma_{aq}} \tag{3}$$

$$\Gamma_{aq} = \frac{4VRTH_{aq}k_{aq}}{S_a\omega} \tag{4}$$

where R_p is the particle radius (m), D_g is the gas-phase diffusion coefficient (0.1 cm^2/s), α is the mass accommodation coefficient (0.1 or higher based on the values of γ_{IEPOX}), V is the total particle volume (cm^3/cm^3), R is the universal gas constant (L atm/mol K), T is temperature (K), H_{aq} is the Henry's law coefficient in the aqueous phase (M/atm), and k_{aq} is the first-order reaction rate constant in the aqueous phase (s^{-1}). The k_{aq} is calculated from Eddingsaas et al.[36]

$$k_{aq} = (k_{H^+}[H^+]) + (k_{nuc}[nuc]a_{H^+}) + k_{ga}[ga] \tag{5}$$

where k_{H^+} is the reaction rate due to acid-catalyzed ring-opening (measured to be 0.036 M^{-1} s^{-1}),[46] $[H^+]$ is the proton concentration (M), a_{H^+} is the proton activity, k_{nuc} is the reaction rate due to the presence of specific nucleophiles (sulfate, nitrate, chloride, etc.) taken to be 2×10^{-4} M^{-1} s^{-1}, [nuc] is the concentration of nucleophiles (M), k_{ga} is the reaction rate due to the presence of general acids (e.g., bisulfate) taken to be 7.3×10^{-4} M^{-1} s^{-1}, and [ga] is the concentration of general acids (M).[36] The concentrations of acids, nucleophiles, and general acids were all modeled for each experimental condition using AIM II.

The resistor model was iterated with different inputs for H_{aq} until model/measurement agreement was achieved for each experiment. Values of H_{aq} spanned 5.0×10^7 to 4.0×10^8 M/atm with an average value of 1.7×10^8 M/atm for sulfate-containing aerosol (ammonium sulfate and ammonium bisulfate), which compares well to the value of 1.3×10^8 M/atm predicted by Eddingsaas et al.[36] Using this value of H_{aq} and eq 5 for k_{aq}, γ_{IEPOX} was predicted using eq 3 for each experiment at different aerosol acidities (Figure 2, black dashed line). The parametrization accurately captures the dependence of γ_{IEPOX} on aerosol acidity with the exception of the results on ammonium sulfate particles. The parametrization predicts $\gamma_{IEPOX} \sim 3.2 \times 10^{-6}$ for ammonium sulfate, which is below our detection limit for a γ measurement.

Suppression by Organic Coatings. Given that organic material comprises a significant fraction of submicron particle mass, we investigated the uptake of *trans*-β-IEPOX onto mixed organic/inorganic particles using ammonium bisulfate as the inorganic component and polyethylene glycol (PEG) as the organic component. PEG was chosen because it has been shown to undergo an RH-dependent liquid–liquid phase separation in the presence of sulfate-containing aerosol forming a coating.[63] This mixture has also been shown to alter the uptake of trace gases in a manner consistent with a PEG coating causing solubility and diffusion limitations at the surface of the particle.[48,62,64,65] At each RH, γ_{IEPOX} decreases with increasing PEG mass fraction (Table 1, Figure 4), but suppression for the same PEG mass fraction was stronger at higher RH. We note

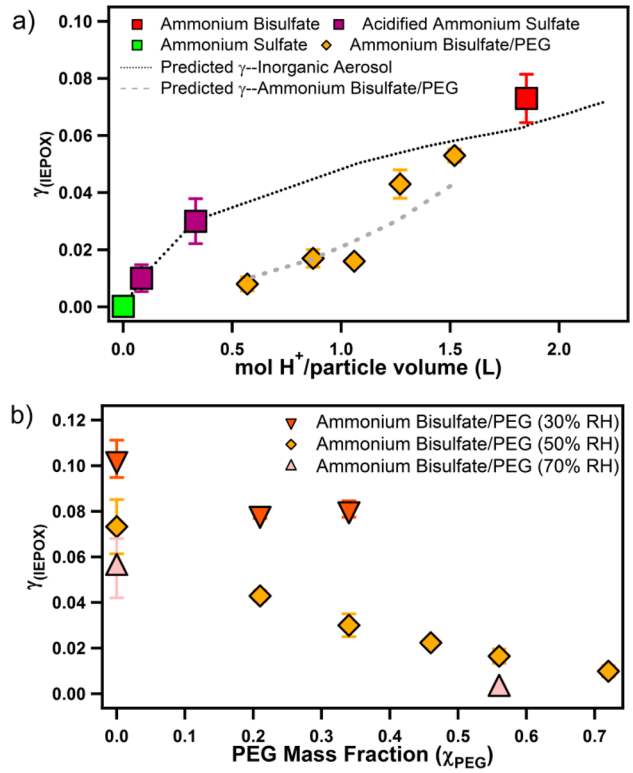

Figure 4. (a) Reactive uptake of *trans*-β-IEPOX as a function of predicted aerosol proton concentration from the AIM II model for ammonium bisulfate (red square), ammonium sulfate acidified to pH 0.5 and 1 (purple squares), ammonium sulfate (green square), and ammonium bisulfate/PEG particles (orange diamonds). Also shown is the predicted reactive uptake assuming the parameters presented in Eddingsaas et al.[36] and using a modified version of the parametrizations presented in Anttila et al.,[62] Bertram and Thornton,[47] and Gaston et al.[48] for inorganic particles (black dotted line) and mixtures of ammonium bisulfate and PEG (gray dashed line). (b) Reactive uptake of *trans*-β-IEPOX on mixed ammonium bisulfate/PEG particles as a function of PEG mass fraction. Measurements are shown at 30% RH (dark orange upside down triangles), 50% RH (orange diamonds), and 70% RH (pink right-side up triangles).

that this RH dependence is opposite to that of N_2O_5 reactivity on mixed PEG/ammonium bisulfate particles.[48] N_2O_5 reactive uptake is likely much more sensitive to diffusion limitations than *trans*-β-IEPOX, given that k_{aq} for $N_2O_5 \sim 1 \times 10^6$ s^{-1} while that for *trans*-β-IEPOX is ~0.1 s^{-1}.

An additional resistance term was added to the parametrization for organic coatings (Γ_{org}) assuming that the ammonium bisulfate/PEG particles have a core–shell morphology with PEG surrounding the ammonium bisulfate core as described in Anttila et al.[62] and Gaston et al.[48]

$$\frac{1}{\gamma} = \frac{R_p\omega}{4D_{gas}} + \frac{1}{\alpha} + \frac{1}{\Gamma_{aq}} + \frac{1}{\Gamma_{org}} \tag{6}$$

where

$$\frac{1}{\Gamma_{org}} = \frac{\omega l_{org}}{4RTH_{org}D_{org}}\frac{R_p}{R_c} \tag{7}$$

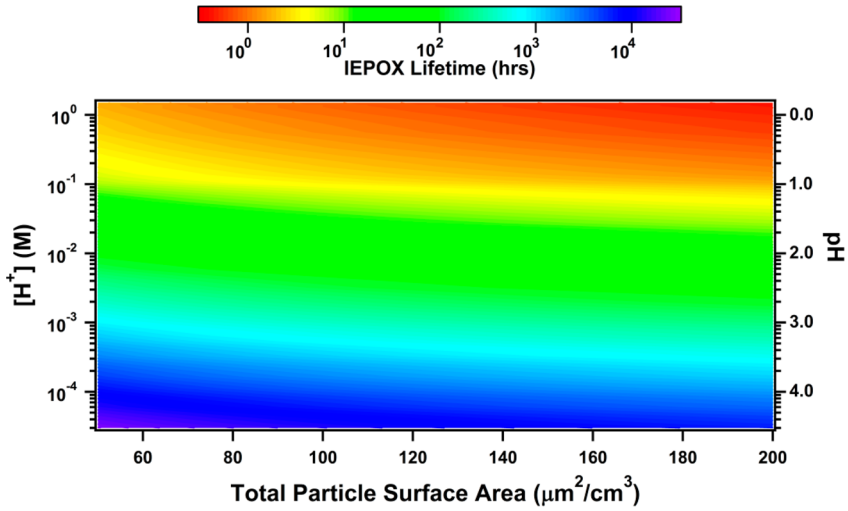

Figure 5. Parameterized IEPOX lifetimes as a function of aerosol acidity and total particle surface area (see text for details of the parametrization). The predicted lifetimes neglect any effect from organic aerosol and/or coatings and, therefore, represent lower limits for the IEPOX lifetime in the presence of aqueous, inorganic aerosol.

In eq 7, l_{org} is the coating thickness, H_{org} is the Henry's law coefficient in the organic layer, D_{org} is the diffusion coefficient in the organic layer, and R_c is the radius of the aqueous core. Based on viscosity measurements of PEG solutions, we estimate D_{org} to be $\sim 1 \times 10^{-10}$ m^2/s for a PEG solution at 50% RH with decreasing viscosity at lower RH due to phase separation.[66,67] Gaston et al.[48] report D_{org} to be only a factor of 2 smaller than that for aqueous solutions (1×10^{-9} m^2/s). Thus, measurement/model agreement requires a combination of reduced diffusivity, mass accommodation, and in particular, greatly reduced partitioning to and/or solubility of *trans*-β-IEPOX in a coating of PEG compared to a concentrated solution of ammonium bisulfate, in terms of Henry's law, $H_{org} \approx 10^{-8} H_{aq}$. The reduction in IEPOX partitioning probably results from the lower proton donor and nucleophilic activity within the PEG coating, with a possible shift to volatility-driven absorptive partitioning. Thus, the addition of organic material and the formation of organic coatings change *trans*-β-IEPOX partitioning and reactivity, thereby affecting γ_{IEPOX}.

Implications for Parameterizations of Isoprene-Derived SOA. Our results indicate that aerosol acidity is the primary factor driving the reactive uptake of *trans*-β-IEPOX over the range of pHs and particle compositions explored in this work. The steepest changes in γ_{IEPOX} are predicted to occur at pH $\leq$ 3 (Figure 2), a value that is not unreasonable for submicron particles close to urban or power plant sources of SO_2 and natural sources of marine biogenic sulfur.[68,69] A lack of correlation between particle acidity and IEPOX-derived SOA in field observations could be due to the titration of ambient aerosol acidity subsequent to IEPOX uptake and/or the presence of organic coatings that could suppress reactive uptake even in the presence of aerosol acidity. Consistent with predictions from bulk solution kinetics,[36,70] we measured the largest change in the reactive uptake of *trans*-β-IEPOX at pH $\leq$ 1, while for pH $\geq$ 1, γ_{IEPOX}, and especially equilibrium partitioning, will be more sensitive to ring-opening chemistry that is not driven by acid catalysis, consistent with the work of Nguyen et al.[44]

Excellent agreement was obtained between our measured and predicted values of γ_{IEPOX} using a resistor model framework with a Henry's law coefficient (H_{aq}) of 1.7×10^8 (M/atm) and a $k_{H^+} \sim 0.036$ M^{-1} s^{-1}, which agree well with the values measured or estimated by Eddingsaas et al.[36] and Cole-Filipiak et al.[46] However, we also provide evidence that the aerosol ionic strength affects the Henry's law partitioning of *trans*-β-IEPOX into the aerosol. The role of different salts and organic material on the ionic strength of the aerosol and its subsequent impact on the Henry's law partitioning of IEPOX should be further explored.

On the basis of the measured reaction probabilities, the atmospheric lifetime of *trans*-β-IEPOX is shorter than 5 h in the presence of highly acidic aqueous aerosol (pH < 1) for a total particle surface area of $\sim$100 $\mu m^2/cm^3$ but greater than $\sim$480 h (20 d) in the presence of aqueous ammonium sulfate. The lifetime could be longer in the presence of ammonium sulfate based on a predicted γ of 10^{-6} using the parametrization shown in Figure 2. Using this parametrization, we illustrate in Figure 5 the large range of IEPOX lifetimes possible on aqueous inorganic particles across typical atmospheric conditions. These estimated lifetimes neglect any potential impact from organic coatings and, therefore, are likely lower bounds on the IEPOX lifetime. Compared to the predicted lifetimes of $\sim$11 h for deposition[36] and $\sim$8 h for gas-phase oxidation at an average OH radical concentration of 1×10^6 molecules/cm^3,[45,70] our results imply that for atmospherically relevant total particle surface areas ($\sim$50−200 $\mu m^2/cm^3$), reactive uptake of IEPOX onto aqueous highly acidic particles (pH $\leq$ 1) would be a competitive or even dominant fate. But IEPOX reactive uptake would not be competitive where ammonia or other alkaline components shift the pH to > $\sim$ 2, which is likely a common situation over much of the Northern Hemisphere.

A recent modeling study improved closure between measured and predicted mass concentrations of SOA, and especially 2-methyltetrols, over the Southeastern U.S. when the reactive uptake of isoprene-derived epoxides was included using an H_{aq} of 2.7×10^6 M/atm and α of 0.02 for IEPOX.[18] Our results suggest H_{aq} and α, and thus γ, are higher than predicted by Pye et al.[18] by orders of magnitude, which could lead to higher predicted yields of IEPOX-derived SOA on a faster time scale, although the SOA yield per reactive uptake of IEPOX has not yet been directly measured. Additionally, our results likely

aid in bringing the modeled and measured total IEPOX-derived SOA mass in closer agreement than recently reported.[71]

Our results represent uptake measured on relatively short time scales (seconds to minutes), but the reactive uptake of IEPOX may change over longer time scales. Preliminary results from the University of North Carolina using a separate but similar apparatus are consistent with ours but also suggest γ_{IEPOX} decreases at time scales longer than probed in this work. One possible reason for this finding is that the IEPOX-derived SOA forms a viscous coating potentially impeding further IEPOX uptake, similar to other biogenic SOA systems,[72,73] and consistent with our measurements on ammonium bisulfate/PEG-mixed particles which provide evidence that phase separations can suppress the reactive uptake of IEPOX. Thus, the results presented herein may only represent the early phase of IEPOX uptake, well before such coatings are formed. Overall, our work supports incorporation of IEPOX reactive uptake as an acidity-dependent SOA source in models, but the potential impact of organic coatings remains an important uncertainty affecting the magnitude of the reaction probability on regional scales.

■ ASSOCIATED CONTENT

Supporting Information

Description and schematic of the experimental setup, a spectrum of IEPOX from the high-resolution time-of-flight chemical ionization mass spectrometer, a description and schematic of the different techniques used to determine γ_{IEPOX}, and experimental results for γ_{IEPOX} on $MgCl_2$ and NaCl particles. This material is available free of charge via the Internet at http://pubs.acs.org/.

■ AUTHOR INFORMATION

Corresponding Author

*E-mail: thornton@atmos.uw.edu. Phone/Fax: 206-543-4010.

Notes

The authors declare no competing financial interest.

■ ACKNOWLEDGMENTS

Funding for this work at the UW was provided by the National Science Foundation through award NSF-CHE-1112414. The UNC group was funded in part by the U.S. Environmental Protection Agency (EPA) through Grant No. 835404. The contents of this publication are solely the responsibility of the grantee and do not necessarily represent the official views of the U.S. EPA. Further, the U.S. EPA does not endorse the purchase of any commercial products or services mentioned in the publication.

■ REFERENCES

(1) Lohmann, U.; Feichter, J. Global indirect aerosol effects: A review. *Atmos. Chem. Phys.* **2005**, *5*, 715−737.

(2) McFiggans, G.; Artaxo, P.; Baltensperger, U.; Coe, H.; Facchini, M. C.; Feingold, G.; Fuzzi, S.; Gysel, M.; Laaksonen, A.; Lohmann, U.; Mentel, T. F.; Murphy, D. M.; O'Dowd, C. D.; Snider, J. R.; Weingartner, E. The effect of physical and chemical aerosol properties on warm cloud droplet activation. *Atmos. Chem. Phys.* **2006**, *6*, 2593−2649.

(3) Poschl, U. Atmospheric aerosols: Composition, transformation, climate and health effects. *Angew. Chem., Int. Ed.* **2005**, *44*, 7520−7540.

(4) Quinn, P. K.; Bates, T. S.; Coffman, D. J.; Covert, D. S. Influence of particle size and chemistry on the cloud nucleating properties of aerosols. *Atmos. Chem. Phys.* **2008**, *8*, 1029−1042.

(5) Jimenez, J. L.; Canagaratna, M. R.; Donahue, N. M.; Prevot, A. S. H.; Zhang, Q.; Kroll, J. H.; DeCarlo, P. F.; Allan, J. D.; Coe, H.; Ng, N. L.; Aiken, A. C.; Docherty, K. S.; Ulbrich, I. M.; Grieshop, A. P.; Robinson, A. L.; Duplissy, J.; Smith, J. D.; Wilson, K. R.; Lanz, V. A.; Hueglin, C.; Sun, Y. L.; Tian, J.; Laaksonen, A.; Raatikainen, T.; Rautiainen, J.; Vaattovaara, P.; Ehn, M.; Kulmala, M.; Tomlinson, J. M.; Collins, D. R.; Cubison, M. J.; Dunlea, E. J.; Huffman, J. A.; Onasch, T. B.; Alfarra, M. R.; Williams, P. I.; Bower, K.; Kondo, Y.; Schneider, J.; Drewnick, F.; Borrmann, S.; Weimer, S.; Demerjian, K.; Salcedo, D.; Cottrell, L.; Griffin, R.; Takami, A.; Miyoshi, T.; Hatakeyama, S.; Shimono, A.; Sun, J. Y.; Zhang, Y. M.; Dzepina, K.; Kimmel, J. R.; Sueper, D.; Jayne, J. T.; Herndon, S. C.; Trimborn, A. M.; Williams, L. R.; Wood, E. C.; Middlebrook, A. M.; Kolb, C. E.; Baltensperger, U.; Worsnop, D. R. Evolution of organic aerosols in the atmosphere. *Science* **2009**, *326*, 1525−1529.

(6) Ng, N. L.; Canagaratna, M. R.; Zhang, Q.; Jimenez, J. L.; Tian, J.; Ulbrich, I. M.; Kroll, J. H.; Docherty, K. S.; Chhabra, P. S.; Bahreini, R.; Murphy, S. M.; Seinfeld, J. H.; Hildebrandt, L.; Donohue, N. M.; DeCarlo, P. F.; Lanz, V. A.; Prevot, A. S. H.; Dinar, E.; Rudich, Y.; Worsnop, D. R. Organic aerosol components observed in Northern Hemispheric datasets from aerosol mass spectrometry. *Atmos. Chem. Phys.* **2010**, *10*, 4625−4641.

(7) Carlton, A. G.; Wiedinmyer, C.; Kroll, J. H. A review of secondary organic aerosol (SOA) formation from isoprene. *Atmos. Chem. Phys.* **2009**, *9*, 4987−5005.

(8) Forster, P.; Ramaswamy, V.; Artaxo, P.; Berntsen, T.; Betts, R.; Fahey, D. W.; Haywood, J.; Lean, J.; Lowe, D. C.; Myhre, G.; Nganga, J.; Prinn, R.; Raga, G.; Schulz, M.; Van Dorland, R. In *Climate Change 2007: The Physical Science Basis. Contribution of Working Group I to the Fourth Assessment Report of the Intergovernmental Panel on Climate Change*; Solomon, S., Qin, D., Manning, M., Chen, Z., Marquis, M., Averyt, K. B., Tignor, M., Miller, H. L., Eds.; Cambridge University Press: Cambridge, 2007.

(9) Hallquist, M.; Wenger, J. C.; Baltensperger, U.; Rudich, Y.; Simpson, D.; Claeys, M.; Dommen, J.; Donahue, N. M.; George, C.; Goldstein, A. H.; Hamilton, J.; Herrmann, H.; Hoffmann, T.; Iinuma, Y.; Jang, M.; Jenkin, M. E.; Jimenez, J. L.; Kiendler-Scharr, A.; Maenhaut, W.; McFiggans, G.; Mentel, T. F.; Monod, A.; Prevot, A. S. H.; Seinfeld, J. H.; Surratt, J. D.; Szmigielski, R.; Wildt, J. The formation, properties and impact of secondary organic aerosol: Current and emerging issues. *Atmos. Chem. Phys.* **2009**, *9*, 5155−5236.

(10) Fuzzi, S.; Andreae, M. O.; Huebert, B. J.; Kulmala, M.; Bond, T. C.; Boy, M.; Doherty, S. J.; Guenther, A.; Kanakidou, M.; Kawamura, K.; Kerminen, V.-M.; Lohmann, U.; Russell, L. M.; Poschl, U. Critical assessment of the current state of scientific knowledge, terminology, and research needs concerning the role of organic aerosols in the atmosphere, climate, and global change. *Atmos. Chem. Phys.* **2006**, *6*, 2017−2038.

(11) Kanakidou, M.; Seinfeld, J. H.; Pandis, S. N.; Barnes, I.; Dentener, F. J.; Facchini, M. C.; Van Dingenen, R.; Ervens, B.; Nenes, A.; Nielsen, C. J.; Swietlicki, E.; Putaud, J. P.; Balkanski, Y.; Fuzzi, S.; Horth, J.; Moortgat, G. K.; Winterhalter, R.; Myhre, C. E. L.; Tsigaridis, K.; Vignati, E.; Stephanou, E. G.; Wilson, J. Organic aerosol and global climate modeling: A review. *Atmos. Chem. Phys.* **2005**, *5*, 1053−1123.

(12) Goldstein, A. H.; Galbaly, I. E. Known and unexplored organic constituents in the Earth's atmosphere. *Environ. Sci. Technol.* **2007**, 1515−1521.

(13) Zhang, Q.; Jimenez, J. L.; Canagaratna, M. R.; Allan, J. D.; Coe, H.; Ulbrich, I. M.; Alfarra, M. R.; Takami, A.; Middlebrook, A. M.; Sun, Y. L.; Dzepina, K.; Dunlea, E.; Docherty, K. S.; DeCarlo, P. F.; Salcedo, D.; Onasch, T. B.; Jayne, J. T.; Miyoshi, T.; Shimono, A.; Hatakeyama, S.; Takegawa, N.; Kondo, Y.; Schneider, J.; Drewnick, F.; Borrmann, S.; Weimer, S.; Demerjian, K.; Williams, P.; Bower, K.; Bahreini, R.; Cottrell, L.; Griffin, R. J.; Rautiainen, J.; Sun, J. Y.; Zhang, Y. M.; Worsnop, D. R. Ubiquity and dominance of oxygenated species in organic aerosols in anthropogenically-influenced Northern Hemisphere midlatitudes. *Geophys. Res. Lett.* **2007**, *34*, L13801.

(14) Dzepina, K.; Volkamer, R. M.; Madronich, S.; Tulet, P.; Ulbrich, I. M.; Zhang, Q.; Cappa, C. D.; Ziemann, P. J.; Jimenez, J. L. Evaluation of recently-proposed secondary organic aerosol models for a case study in Mexico City. *Atmos. Chem. Phys.* **2009**, *9*, 5681−5709.
(15) Heald, C. L.; Jacob, D. J.; Park, R. J.; Russell, L. M.; Huebert, B. J.; Seinfeld, J. H.; Liao, H.; Weber, R. J. A large organic aerosol source in the free troposphere missing from current models. *Geophys. Res. Lett.* **2005**, *32*, L18809.
(16) Volkamer, R.; Jimenez, J. L.; San Martini, F.; Dzepina, K.; Zhang, Q.; Salcedo, D.; Molina, L. T.; Worsnop, D. R.; Molina, M. J. Secondary organic aerosol formation from anthropogenic air pollution: Rapid and higher than expected. *Geophys. Res. Lett.* **2006**, *33*, L17811.
(17) Ehn, M.; Thornton, J. A.; Kleist, E.; Sipila, M.; Junninen, H.; Pullinen, I.; Springer, M.; Rubach, F.; Tillmann, R.; Lee, B.; Lopez-Hilfiker, F. D.; Andres, S.; Acir, I.-H.; Rissanen, M.; Jokinen, T.; Schobesberger, S.; Kangasluoma, J.; Kontkanen, J.; Nieminen, T.; Kurten, T.; Nielsen, L. B.; Jorgensen, S.; Kjaergaard, H. G.; Canagaratna, M. R.; Dal Maso, M.; Berndt, T.; Petaja, T.; Wahner, A.; Kerminen, V.-M.; Kulmala, M.; Worsnop, D. R.; Wildt, J.; Mentel, T. F. A large source of low-volatility secondary organic aerosol. *Nature* **2014**, *506*, 476−479.
(18) Pye, H. O. T.; Pinder, R. W.; Piletic, I. R.; Xie, Y.; Capps, S. L.; Lin, Y.-H.; Surratt, J. D.; Zhang, Z.; Gold, A.; Luecken, D. J.; Hutzell, W. T.; Jaoui, M.; Offenberg, J. H.; Kleindienst, T. E.; Lewandowski, M.; Edney, E. O. Epoxide pathways improve model predictions of isoprene markers and reveal key role of acidity in aerosol formation. *Environ. Sci. Technol.* **2013**, DOI: 10.1021/es402106h.
(19) Riipinen, I.; Pierce, J. R.; Yli-Juuti, T.; Nieminen, T.; Hakkinen, S.; Ehn, M.; Junninen, H.; Lehtipalo, K.; Petaja, T.; Slowik, J. G.; Chang, R.; Shantz, N. C.; Abbatt, J.; Leaitch, W. R.; Kerminen, V.-M.; Worsnop, D. R.; Pandis, S. N.; Donahue, N. M.; Kulmala, M. Organic condensation: A vital link connecting aerosol formation to cloud condensation nuclei (CCN) concentrations. *Atmos. Chem. Phys.* **2011**, *11*, 3865−3878.
(20) Spracklen, D. V.; Jimenez, J. L.; Carslaw, K. S.; Worsnop, D. R.; Evans, M. J.; Mann, G. W.; Zhang, Q.; Canagaratna, M. R.; Allan, J. D.; Coe, H.; McFiggans, G.; Rap, A.; Forster, P. Aerosol mass spectrometer constraint on the global secondary organic aerosol budget. *Atmos. Chem. Phys.* **2011**, *11*, 12109−12136.
(21) Schichtel, B. A.; Malm, W. C.; Bench, G.; Fallon, S.; McDade, C. E.; Chow, J. C.; Watson, J. G. Fossil and contemporary fine particulate carbon fractions at 12 rural and urban sites in the United States. *J. Geophys. Res.* **2008**, *113*, D02311.
(22) Guenther, A.; Karl, T.; Harley, P.; Wiedinmyer, C.; Palmer, P. I.; Geron, C. Estimates of global terrestrial isoprene emissions using MEGAN (model of emissions of gases and aerosols from nature). *Atmos. Chem. Phys.* **2006**, *6*, 3181−3210.
(23) Claeys, M.; Graham, B.; Vas, G.; Wang, W.; Vermeylen, R.; Pashynska, V.; Cafmeyer, J.; Guyon, P.; Andreae, M. O.; Artaxo, P.; Maenhaut, W. Formation of secondary organic aerosols through photooxidation of isoprene. *Science* **2004**, *303*, 1173−1176.
(24) Kroll, J. H.; Ng, N. L.; Murphy, S. M.; Flagan, R. C.; Seinfeld, J. H. Secondary organic aerosol formation from isoprene photooxidation. *Environ. Sci. Technol.* **2006**, *40*, 1869−1877.
(25) Surratt, J. D.; Murphy, S. M.; Kroll, J. H.; Ng, N. L.; Hildebrandt, L.; Sorooshian, A.; Szmigielski, R.; Vermeylen, R.; Maenhaut, W.; Claeys, M.; Flagan, R. C.; Seinfeld, J. H. Chemical composition of secondary organic aerosol formed from the photooxidation of isoprene. *J. Phys. Chem. A* **2006**, *110*, 9665−9690.
(26) Paulot, F.; Crounse, J. D.; Kjaergaard, H. G.; Kurten, A.; St. Clair, J. M.; Seinfeld, J. H.; Wennberg, P. O. Unexpected epoxide formation in the gas-phase photooxidation of isoprene. *Science* **2009**, *325*, 730−733.
(27) Budisulistiorini, S. H.; Canagaratna, M. R.; Croteau, P. L.; Marth, W. J.; Baumann, K.; Edgerton, E. S.; Shaw, S. L.; Knipping, E. M.; Worsnop, D. R.; Jayne, J. T.; Gold, A.; Surratt, J. D. Real-time continuous characterization of secondary organic aerosol derived from isoprene epoxydiols in downtown Atlanta, Georgia, using the Aerodyne aerosol chemical speciation monitor. *Environ. Sci. Technol.* **2013**, *47*, 5686−5694.
(28) Chan, M. N.; Surratt, J. D.; Claeys, M.; Edgerton, E. S.; Tanner, R. L.; Shaw, S. L.; Zheng, M.; Knipping, E. M.; Eddingsaas, N. C.; Wennberg, P. O.; Seinfeld, J. H. Characterization and quantification of isoprene-derived epoxydiols in ambient aerosol in the southeastern United States. *Environ. Sci. Technol.* **2010**, *44*, 4590−4596.
(29) Hatch, L. E.; Creamean, J. M.; Ault, A. P.; Surratt, J. D.; Chan, M. N.; Seinfeld, J. H.; Edgerton, E. S.; Su, Y.; Prather, K. A. Measurements of isoprene-derived organosulfates in ambient aerosols by aerosol time-of-flight mass spectrometry - Part 1: Single particle atmospheric observations in Atlanta. *Environ. Sci. Technol.* **2011**, *45*, 5105−5111.
(30) Lin, Y.-H.; Zhang, Z.; Docherty, K. S.; Zhang, H.; Budisulistiorini, S. H.; Rubitschun, C. L.; Shaw, S. L.; Knipping, E. M.; Edgerton, E. S.; Kleindienst, T. E.; Gold, A.; Surratt, J. D. Isoprene epoxydiols as precursors to secondary organic aerosol formation: Acid-catalyzed reactive uptake studies with authentic compounds. *Environ. Sci. Technol.* **2012**, *46*, 250−258.
(31) Surratt, J. D.; Chan, A. W.; Eddingsaas, N. C.; Chan, M. N.; Loza, C. L.; Kwan, A. J.; Hersey, S. P.; Flagan, R. C.; Wennberg, P. O.; Seinfeld, J. H. Reactive intermediates revealed in secondary organic aerosol formation from isoprene. *Proc. Natl. Acad. Sci. U.S.A.* **2010**, *107*, 6640−6645.
(32) Surratt, J. D.; Lewandowski, M.; Offenberg, J. H.; Jaoui, M.; Kleindienst, T. E.; Edney, E. O.; Seinfeld, J. H. Effect of acidity on secondary organic aerosol formation from isoprene. *Environ. Sci. Technol.* **2007**, *41*, 5363−5369.
(33) Robinson, N. H.; Hamilton, J. F.; Allan, J. D.; Langford, B.; Oram, D. E.; Chen, Q.; Docherty, K. S.; Farmer, D. K.; Jimenez, J. L.; Ward, M. W.; Hewitt, C. N.; Barley, M. H.; Jenkin, M. E.; Rickard, A. R.; Martin, S. T.; McFiggans, G.; Coe, H. Evidence for a significant proportion of secondary organic aerosol from isoprene above a maritime tropical forest. *Atmos. Chem. Phys.* **2011**, *11*, 1039−1050.
(34) Pratt, K. A.; Fiddler, M. N.; Shepson, P. B.; Carlton, A. G.; Surratt, J. D. Organosulfates in cloud water above the Ozarks' isoprene source region. *Atmos. Environ.* **2013**, *77*, 231−238.
(35) Surratt, J. D.; Kroll, J. H.; Edney, E. O.; Claeys, M.; Sorooshian, A.; Ng, N. L.; Offenberg, J. H.; Lewandowski, M.; Jaoui, M.; Flagan, R. C.; Seinfeld, J. H. Evidence for organosulfates in secondary organic aerosol. *Environ. Sci. Technol.* **2007**, *41*, 517−527.
(36) Eddingsaas, N. C.; VanderVelde, D. G.; Wennberg, P. O. Kinetics and products of the acid-catalyzed ring-opening of atmospherically relevant butyl epoxy alcohols. *J. Phys. Chem. A* **2010**, *114*, 8106−8113.
(37) Minerath, E. C.; Schultz, M. P.; Elrod, M. J. Kinetics of the reactions of isoprene-derived epoxides in model tropospheric aerosol solutions. *Environ. Sci. Technol.* **2009**, *43*, 8133−8139.
(38) Lin, Y.-H.; Knipping, E. M.; Edgerton, E. S.; Shaw, S. L.; Surratt, J. D. Investigating the influences of SO_2 and NH_3 levels on isoprene-derived secondary organic aerosol formation using conditional sampling approaches. *Atmos. Chem. Phys.* **2013**, *13*, 8457−8470.
(39) Worton, D. R.; Surratt, J. D.; LaFranchi, B. W.; Chan, A. W. H.; Zhao, Y.; Weber, R. J.; Park, J.-H.; Gilman, J. B.; de Gouw, J. A.; Park, C.; Schade, G. W.; Beaver, M.; St. Clair, J. M.; Crounse, J. D.; Wennberg, P. O.; Wolfe, G. M.; Harrold, S.; Thornton, J. A.; Farmer, D. K.; Docherty, K. S.; Cubison, M. J.; Jimenez, J. L.; Frossard, A. A.; Russell, L. M.; Kristensen, K.; Glasius, M.; Mao, J.; Ren, X.; Brune, W.; Browne, E. C.; Pusede, S. E.; Cohen, R. C.; Seinfeld, J. H.; Goldstein, A. H. Observational insights into aerosol formation from isoprene. *Environ. Sci. Technol.* **2013**, *47*, 11403−11413.
(40) Koutrakis, P.; Thompson, K. M.; Wolfson, J. M.; Spengler, J. D.; Keeler, G. J.; Slater, J. L. Determination of aerosol strong acidity losses due to interactions of collected particles: Results from laboratory and field studies. *Atmos. Environ.* **1992**, *26A*, 987−995.
(41) Liggio, J.; Li, S.-M.; McLaren, R. Reactive uptake of glyoxal by particulate matter. *J. Geophys. Res.* **2005**, *110*, D10304.

(42) Lim, H.-J.; Carlton, A. G.; Turpin, B. J. Isoprene forms secondary organic aerosol through cloud processing: Model simulations. *Environ. Sci. Technol.* **2005**, *39*, 4441−4446.
(43) Lim, Y. B.; Tan, Y.; Perri, M. J.; Seitzinger, S. P.; Turpin, B. J. Aqueous chemistry and its role in secondary organic aerosol (SOA) formation. *Atmos. Chem. Phys.* **2010**, *10*, 10521−10539.
(44) Nguyen, T. B.; Coggon, M. M.; Bates, K. H.; Zhang, X.; Schwantes, R. H.; Schilling, K. A.; Loza, C. L.; Flagan, R. C.; Wennberg, P. O.; Seinfeld, J. H. Organic aerosol formation from the reactive uptake of isoprene epoxydiols (IEPOX) onto non-acidified inorganic seeds. *Atmos. Chem. Phys.* **2014**, *14*, 3497−3510.
(45) Bates, K. H.; Crounse, J. D.; St. Clair, J. M.; Bennett, N. B.; Nguyen, T. B.; Seinfeld, J. H.; Stoltz, B. M.; Wennberg, P. O. Gas phase production and loss of isoprene epoxydiols. *J. Phys. Chem. A* **2014**, *118*, 1237−1246.
(46) Cole-Filipiak, N. C.; O'Connor, A. E.; Elrod, M. J. Kinetics of the hydrolysis of atmospherically relevant isoprene-derived hydroxy epoxides. *Environ. Sci. Technol.* **2010**, *44*, 6718−6723.
(47) Bertram, T. H.; Thornton, J. A. Toward a general parameterization of N_2O_5 reactivity on aqueous particles: the competing effects of particle liquid water, nitrate and chloride. *Atmos. Chem. Phys.* **2009**, *9*, 8351−8363.
(48) Gaston, C. J.; Thornton, J. A.; Ng, N. L. Reactive uptake of N_2O_5 to internally mixed inorganic and organic particles: The role of organic carbon oxidation state and inferred organic phase separations. *Atmos. Chem. Phys.* **2014**, *14*, 5693−5707.
(49) Lopez-Hilfiker, F. D.; Constantin, K.; Kercher, J. P.; Thornton, J. A. Temperature dependent halogen activation by N_2O_5 reactions on halide-doped ice surfaces. *Atmos. Chem. Phys.* **2012**, *12*, 5237−5247.
(50) McNeill, V. F.; Patterson, J.; Wolfe, G. M.; Thornton, J. A. The effect of varying levels of surfactant on the reactive uptake of N_2O_5 to aqueous aerosol. *Atmos. Chem. Phys.* **2006**, *6*, 1635−1644.
(51) Thornton, J. A.; Braban, C. F.; Abbatt, J. P. D. N_2O_5 hydrolysis on sub-micron organic aerosols: the effect of relative humidity, particle phase, and particle size. *Phys. Chem. Chem. Phys.* **2003**, *5*, 4593−4603.
(52) Clegg, S. L.; Brimblecombe, P.; Wexler, A. S. A thermodynamic model of the system H^+-NH_4^+-SO_4^{2-}-NO_3^--H_2O at tropospheric temperatures. *J. Phys. Chem. A* **1998**, *102*, 2137−2154.
(53) Zhang, Z.; Lin, Y.-H.; Surratt, J. D.; Ball, L. M.; Gold, A. Technical Note: Synthesis of isoprene atmospheric oxidation products: isomeric epoxydiols and the rearrangement products *cis*- and *trans*-3-methyl-3,4-dihydroxytetrahydrofuran. *Atmos. Chem. Phys.* **2012**, *12*, 8529−8535.
(54) Kercher, J. P.; Riedel, T. P.; Thornton, J. A. Chlorine activation by N_2O_5: Simultaneous, in situ detection of $ClNO_2$ and N_2O_5 by chemical ionization mass spectrometry. *Atmos. Meas. Technol.* **2009**, *2*, 193−204.
(55) Lee, B. H.; Lopez-Hilfiker, F. D.; Mohr, C.; Kurten, T. C.; Worsnop, D.; Thornton, J. A. An iodide-adduct high-resolution time-of-flight chemical-ionization mass spectrometer: Application to atmospheric inorganic and organic compounds. *Environ. Sci. Technol.* **2014**, *48*, 6309−6317.
(56) Bertram, T. H.; Thornton, J. A.; Riedel, T. P. An experimental technique for the direct measurement of N_2O_5 reactivity on ambient particles. *Atmos. Meas. Technol.* **2009**, *2*, 231−242.
(57) Fuchs, N. A.; Sutugin, A. G. In *Topics in Current Aerosol Research*; Hidy, G. M., Brock, J. R., Eds.; Pergamon Press: New York, 1971; pp 1−60.
(58) Brown, R. L. Tubular flow reactors with 1st-order kinetics. *J. Res. Nat. Bureau Stand.* **1978**, *83*, 1−8.
(59) Ip, H. S. S.; Huang, X. H. H.; Yu, J. Z. Effective Henry's law constants of glyoxal, glyoxylic acid, and glycolic acid. *Geophys. Res. Lett.* **2009**, DOI: 10.1029/2008GL036212.
(60) Kampf, C. J.; Waxman, E. M.; Slowik, J. G.; Dommen, J.; Pfaffenberger, L.; Praplan, A. P.; Prevot, A. S. H.; Baltensperger, U.; Hoffmann, T.; Volkamer, R. Effective Henry's law partitioning and the salting constant of glyoxal in aerosols containing sulfate. *Environ. Sci. Technol.* **2013**, *47*, 4236−4244.
(61) Casillas-Ituarte, N. N.; Callahan, K. M.; Tang, C. Y.; Chen, X.; Roeselová, M.; Tobias, D. J.; Allen, H. C. Surface organization of aqueous $MgCl_2$ and application to atmospheric marine aerosol chemistry. *Proc. Natl. Acad. Sci. U.S.A.* **2010**, 6616−6621.
(62) Anttila, T.; Kiendler-Scharr, A.; Tillmann, R.; Mentel, T. F. On the reactive uptake of gaseous compounds by organic-coated aqueous aerosols: Theoretical analysis and application to the heterogeneous hydrolysis of N_2O_5. *J. Phys. Chem. A* **2006**, *110*, 10435−10443.
(63) Ciobanu, V. G.; Marcolli, C.; Krieger, U. K.; Weers, U.; Peter, T. Liquid−liquid phase separation in mixed organic/inorganic aerosol particles. *J. Phys. Chem. A* **2009**, *113*, 10966−10978.
(64) Bertram, A. K.; Martin, S. T.; Hanna, S. J.; Smith, M. L.; Bodsworth, A.; Chen, Q.; Kuwata, M.; Liu, A.; You, Y.; Zorn, S. R. Predicting the relative humidities of liquid-liquid phase separation, efflorescence, and deliquescence of mixed particles of ammonium sulfate, organic material, and water using the organic-to-sulfate mass ratio of the particle and the oxygen-to-carbon elemental ratio of the organic component. *Atmos. Chem. Phys.* **2011**, *11*, 10995−11006.
(65) Riemer, N.; Vogel, H.; Vogel, B.; Anttila, T.; Kiendler-Scharr, A.; Mentel, T. F. Relative importance of organic coatings for the heterogeneous hydrolysis of N_2O_5 during summer in Europe. *J. Geophys. Res.* **2009**, *114*, D17307.
(66) Ninni, L.; Burd, H.; Fung, W. H.; Meirelles, A. J. A. Kinematic viscosites of poly(ethylene glycol) aqueous solutions. *J. Chem. Eng. Data* **2003**, *48*, 324−329.
(67) Rahbari-Sisakht, M.; Taghizadeh, M.; Eliassi, A. Densities and viscosities of binary mixtures of poly(ethylene glycol) and poly-(propylene glycol) in water and ethanol in the 293.15−338.15 K temperature range. *J. Chem. Eng. Data* **2003**, *48*, 1221−1224.
(68) Keene, W. C.; Sander, R.; Pszenny, A. A. P.; Vogt, R.; Crutzen, P. J.; Galloway, J. N. Aerosol pH in the marine boundary layer: A review and model evaluation. *J. Aerosol Sci.* **1998**, *19*, 339−356.
(69) Zhang, Q.; Jimenez, J. L.; Worsnop, D. R.; Canagaratna, M. R. A case study of urban particle acidity and its influence on secondary organic aerosol. *Environ. Sci. Technol.* **2007**, *41*, 3213−3219.
(70) Jacobs, M. I.; Darer, A. I.; Elrod, M. J. Rate constants and products of the OH reaction with isoprene-derived epoxides. *Environ. Sci. Technol.* **2013**, *47*, 12868−12876.
(71) Karambelas, A.; Pye, H. O. T.; Budisulistiorini, S. H.; Surratt, J. D.; Pinder, R. W. Contribution of isoprene epoxydiol to urban organic aerosol: Evidence from modeling and measurements. *Environ. Sci. Technol. Lett.* **2014**, *1*, 278−283.
(72) Drozd, G. T.; Woo, J. L.; McNeill, V. F. Self-limited uptake of α-pinene oxide to acidic aerosol: The effects of liquid-liquid phase separation and implications for the formation of secondary organic aerosol and organosulfates from epoxides. *Atmos. Chem. Phys.* **2013**, *13*, 8255−8263.
(73) Virtanen, A.; Joutsensaari, J.; Koop, T.; Kannosto, J.; Yli-Pirila, P.; Leskinen, J.; Makela, J. M.; Holopainen, J. K.; Poschl, U.; Kulmala, M.; Worsnop, D. R.; Laaksonen, A. An amorphous solid state of biogenic secondary organic aerosol particles. *Nature* **2010**, *467*, 824−827.